Toxicology in Vitro 30 (2015) 250–263

Contents lists available at ScienceDirect

Toxicology in Vitro

journal homepage: www.elsevier.com/locate/tiv

Antiproliferative activity of goniothalamin enantiomers involves DNA damage, cell cycle arrest and apoptosis induction in MCF-7 and HB4a cells

Simone Cristine Semprebon [a,*], Lilian Areal Marques [a], Gláucia Fernanda Rocha D'Epiro [a], Elaine Aparecida de Camargo [b], Glenda Nicioli da Silva [b], Andressa Megumi Niwa [a], Fernando Macedo Junior [c], Mário Sérgio Mantovani [a]

[a] Departamento de Biologia Geral, Universidade Estadual de Londrina, Londrina, PR, Brazil
[b] Departamento de Patologia, Universidade Estadual Paulista Júlio Mesquita Filho, Botucatu, SP, Brazil
[c] Departamento de Química, Universidade Estadual de Londrina, Londrina, PR, Brazil

ARTICLE INFO

Article history:
Received 27 May 2015
Received in revised form 20 August 2015
Accepted 12 October 2015
Available online 29 October 2015

Keywords:
Goniothalamin
Genotoxicity
Cyclins
CDKs
Cell cycle arrest
Apoptosis

ABSTRACT

(R)-goniothalamin (R-GNT) is a styryl lactone that exhibits antiproliferative property against several tumor cell lines. (S)-goniothalamin (S-GNT) is the synthetic enantiomer of R-GNT, and their biological properties are poorly understood. The aim of this study was to evaluate the antiproliferative mechanisms of (R)-goniothalamin and (S)-goniothalamin in MCF-7 breast cancer cells and HB4a epithelial mammary cells. To determine the mechanisms of cell growth inhibition, we analyzed the ability of R-GNT and S-GNT to induce DNA damage, cell cycle arrest and apoptosis. Moreover, the gene expression of cell cycle components, including cyclin, CDKs and CKIs, as well as of genes involved in apoptosis and the DNA damage response were evaluated. The natural enantiomer R-GNT proved more effective in both cell lines than did the synthetic enantiomer S-GNT, inhibiting cell proliferation via cell cycle arrest and apoptosis induction, likely in response to DNA damage. The cell cycle inhibition caused by R-GNT was mediated through the upregulation of CIP/KIP cyclin-kinase inhibitors and through the downregulation of cyclins and CDKs. S-GNT, in turn, was able to cause G0/G1 cell cycle arrest and DNA damage in MCF-7 cells and apoptosis induction only in HB4a cells. Therefore, goniothalamin presents potent antiproliferative activity to breast cancer cells MCF-7. However, exposure to goniothalamin brings some undesirable effects to non-tumor cells HB4a, including genotoxicity and apoptosis induction.

1. Introduction

Breast cancer is the second most common cancer among women worldwide. Although breast cancer exhibits good prognosis, mortality rates remain high. In developed countries, the average survival rate at 5 years is 85%, whereas the survival rate in developing countries is approximately 60% (WHO, 2012). Of all breast cancer patients, approximately 20–30% develop metastatic disease and exhibit an average survival between 2 and 4 years depending of the subtype of the disease (Eroles et al., 2012). Therefore, new therapeutic strategies with fewer side effects, greater selectivity and a more effective response are required.

Several natural compounds with potent cytotoxic effects have been used as anticancer drugs. One such molecule obtained from natural source with potent antiproliferative activity is goniothalamin (GNT), a styryl lactone found in members of the family Annonaceae, in the *Goniothalamus* sp. (Wiart, 2007). The *R* configuration (Right) is accepted as the absolute configuration of this molecule in its natural form. (S)-goniothalamin is the synthetic form of this molecule (Fatima et al., 2006).

Among all of the bioactive properties of goniothalamin that have been described, one of the most notable is its anti-proliferative activity against various tumor cell lines, including breast cancer (Alabsi et al., 2012; Chen et al., 2005; de Fatima et al., 2005; Wattanapiromsakul et al., 2005), liver cancer (Al-Qubaisi et al., 2011; Tian et al., 2006), leukemic cells (Inayat-Hussain et al., 1999; Inayat-Hussain et al., 2009; Petsophonsakul et al., 2013; Rajab et al., 2005), colon cancer (Alabsi et al., 2012; de Fatima et al., 2005; Wattanapiromsakul et al., 2005), lung cancer (de Fatima et al., 2005; Semprebon et al., 2014; Wattanapiromsakul et al., 2005), kidney cancer (de Fatima et al., 2008; Wattanapiromsakul et al., 2005), ovarian and prostate cancer (de Fatima et al., 2005). Furthermore, the synthetic enantiomer, (S)-goniothalamin, also exhibits antiproliferative potential (de Fatima et al., 2008; Fatima et al., 2006; Semprebon et al., 2014), but its mechanism of action remains poorly understood. (R)-goniothalamin (R-GNT) and (S)-goniothalamin (S-GNT) reportedly exhibit antitumor activity in Ehrlich solid tumors without evidence of toxicity or weight loss in the experimental animals (Vendramini-Costa et al., 2010). Several reports suggest that induction of the intrinsic apoptosis pathway is the primary

* Corresponding author at: Departamento de Biologia Geral — CCB, Universidade Estadual de Londrina — Campus Universitário, P.O. Box 6001, Londrina, Paraná CEP: 86051-990, Brazil.
E-mail address: sc.semprebon@gmail.com (S.C. Semprebon).

http://dx.doi.org/10.1016/j.tiv.2015.10.012
0887-2333/

mechanism by which (R)-goniothalamin exert its antiproliferative activity in vitro (Alabsi et al., 2013; Barcelos et al., 2014; Kuo et al., 2011; Petsophonsakul et al., 2013). However, little is known about its effects on the cell cycle.

The cell cycle machinery promotes the progression of the cell from a quiescent state (G0) to a proliferative state while ensuring genomic fidelity. The cyclin-dependent kinases (CDKs) associate with cyclins to drive the progression of the cell through the cell cycle. CDKs 4, 6, 2 and 1 phosphorylate proteins responsible for cell cycle events. The cyclic changes in the activities of these complexes are regulated by cyclins (D, E, A and B). Mitogenic stimuli cause the accumulation of cyclin D1. The complex of this cyclin with CDK4/6 phosphorylates the Rb protein. Rb phosphorylation causes its dissociation of E2F, a transcriptional factor that regulates the expression of genes that encode components of subsequent cell cycle events, such as cyclins E, A and B1 and CDK1, among others. The next cyclin to be induced is cyclin E, which associates with CDK2 to promote the G1–S transition. The cyclin A/CDK2 complex is required for the entry and completion of S phase, and cyclin A associates with CDK1 promote entry into M phase. Mitosis, in turn, is regulated by the cyclin B/CDK1 complex (Malumbres and Barbacid, 2005). Cyclin-kinase inhibitors (CKIs) can counteract CDK activity. The CIP/KIP family of CKIs includes p21, p27 and p57 (Romanov et al., 2012). *CDKN1A* is a transcriptional target of p53 that encodes the $p21^{Kip1}$ protein (Gartel and Tyner, 1999; Macleod et al., 1995). This protein can inhibit the cell cycle progression at G1, S (Besson et al., 2008) and G2/M phases (Lee et al., 2009).

The malignant phenotype results from the manifestation of essential alterations in cell physiology that allow cancer cells survive, proliferate and spread, such as sustained proliferative signaling, evasion of growth suppressors and resistance of cell death, among others (Hanahan and Weinberg, 2011). Genetic alterations in regulators of CDKs such as cyclins and CKIs, or in its substrates such as the Rb protein are common in human cancer (Malumbres and Barbacid, 2005). Therefore, compounds with the ability to modulate the cell cycle machinery and induce cell cycle arrest and apoptosis can be good targets for cancer treatment. In this context, the aim of this study was evaluate the antiproliferative mechanisms of (R)-goniothalamin and (S)-goniothalamin in breast cancer MCF-7 cells and epithelial mammary HB4a cells, comparing their effects in tumoral and non-tumoral cells. To determine the mechanisms of cell growth inhibition, we analyzed the ability of R-GNT and S-GNT in induce DNA damage, cell cycle arrest and apoptosis. Moreover, the gene expression of cell cycle components, such as cyclins, CDKs and CKIs, as well as genes involved in the DNA damage response (*GADD45a*) and apoptosis (*CASP8* and *CASP9*) were evaluated. Our study provides novel insight into the role of goniothalamin as a cell cycle regulator in breast cells.

2. Materials and methods

2.1. Chemicals

(R)-goniothalamin (R-GNT) and (S)-goniothalamin (S-GNT) (Fig. 1) were synthesized in the Laboratório de Pesquisas de Moléculas Bioativas (LPMBA) of the Departamento de Química da Universidade Estadual de Londrina (UEL) in collaboration with the Prof. Dr. Ângelo de Fátima of Departamento de Química da Universidade Federal de Minas Gerais (UFMG), as previously described (Fatima et al., 2006). The test substance was solubilized in dimethylsulfoxide (DMSO) (Mallinckrodt Chemicals, USA) at a concentration of 20.000 μM and stored at −20 °C. Upon use, the solution was diluted in culture medium at experimental concentrations. The composition of the GNT solutions was monitored through the study by high resolution 1 H NMR (Bruker spectrometer, Model Avance III) which showed that the test compounds had been intact at above 97.5% purity. The DMSO concentration did not exceed 0.5% in culture. The control group received the amount of DMSO equivalent to the treated group. The chemotherapeutic agent doxorubicin (Zodiac, Brazil) was used at concentration of 1 μM as a positive control.

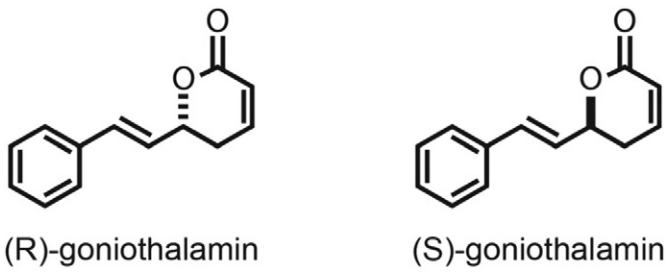

Fig. 1. Chemical structures of (R)-goniothalamin and (S)-goniothalamin.

2.2. Cell culture

The human breast adenocarcinoma MCF-7 cell line was obtained from Cell Bank of the Universidade Federal do Rio de Janeiro (BCRJ/UFRJ), and the normal mammary epithelial HB4a cell line was kindly provided by AC Camargo Hospital (SP). These cell lines were cultured in Dulbecco's Modified Eagle Medium (DMEM) (Gibco®, Life Technologies, USA) supplemented with 10% fetal bovine serum (FBS, Gibco®) and 1% penicillin/streptomycin (Gibco®) and maintained in a humidified incubator containing 5% CO_2 at 37 °C. The HB4a cell line was also supplemented with 5 μg/ml of insulin (Gibco®) and 5 mg/ml of hydrocortisone. Under these conditions, the cell viability remained >90%.

2.3. Cell viability assay

The cell viability assay was based on the conversion of MTT [3-(4,5-dimethylthiazol-2-yl)-2,5-diphenyltetrazolium bromide] (Invitrogen Life Technologies, USA) to formazan crystals by mitochondrial dehydrogenase in living cells, as described by Mosmann (1983) with some modifications. Exponentially growing cells were seeded in 96-well plates at a density of 5×10^3 cells/well in 100 μL of culture medium. After 24 h of incubation, R-GNT and S-GNT (1, 10, 20, 30, 40, 50, 100 and 150 μM) were added and remained in culture for 24 h and 48 h. After exposure, the treatments were removed, and 100 μL of MTT reagent (0.5 mg/ml) was added to each well and kept at 37 °C for 4 h to form formazan crystals. The cell culture medium was aspirated, and 100 μL of DMSO was added to dissolve the crystals. The absorbance was measured at 570 nm using a spectrophotometer (Thermo Plate). Assays were performed in four replicates and three experiments. Cell viability (CV) was expressed as a percentage of the negative control.

2.4. Real-time cell growth kinetics xCELLigence

The real-time growth kinetics of the cells was examined by an impedance-based Real-Time Cell Analysis (RTCA) system xCELLigence (Roche Diagnostic, Germany). This system monitors the cell biological status through impedance measurements. Alterations in cellular biological status, including the number of cells, cell viability, morphology and adhesion, change the impedance values, which are expressed through the Cell Index (CI), as produced by xCELLigence. Changes in impedance are proportional to the number of cells in the well, the morphological changes and adhesion. Thus, larger cell numbers are reflected in greater impedance values (Xing et al., 2005). The RTCA station remained in a humidified incubator containing 5% CO_2 at 37 °C. Briefly, 50 μL of medium was added to the 96-well E-plate, and background readings were recorded. The cells were seeded at a density of 6250 MCF-7 cells/well or 3125 HB4a cells/well, according to data obtained in the titration experiment. The E-plate containing the cells was incubated at room temperature for 30 min and thereafter placed in the RTCA station. After 24 h, when the cells were in a logarithmic growth phase, 100 μL R-GNT and S-GNT (1, 10, 20, 30, 40, 50 and 100 μM) were added and kept in culture

for 96 h. The impedance was monitored every 30 min for 96 h. The experiment was designed according to the manufacturer's recommendations and was performed in triplicate. The cell growth curves were normalized to the Cell Index (CI) at the last time point before treatment addition using the RTCA software (Roche Diagnostic, Germany).

2.5. Cell cycle analysis

Briefly, cells were seeded in 6-well plates at a density of 10^5 cells/well. After 24 h of incubation, R-GNT and S-GNT (10 and 50 μM) were added. After 3 h and 24 h of exposure, cells were trypsinized, resuspended in DMEM and centrifuged for 5 min. The cell suspension was resuspended in 100 μL HFS (50 mg/mL propidium iodide, 0.1% sodium citrate, 0.1% Triton X-100) (Sigma Aldrich, USA) and incubated for 30 min. After staining, the DNA content based on the fluorescence intensity of PI was estimated by flow cytometry (Guava easyCyte™, Millipore, USA). The data were analyzed using a Guava software (Millipore, USA). The percentages of cells in different phases of the cycle (G1, S and G2/M) as well as the percentage of cells with fragmented DNA (sub-G1 region) were estimated. For each sample examined, 5000 events were analyzed in three experiments.

2.6. Apoptosis assay

The apoptosis-inducing potential analyses of R and S-GNT were performed using an annexin V assay kit (Guava Nexin®, Millipore, USA). The cells were seeded in 6-well plates at a density of 10^5 cells/well. After 24 h of incubation, R-GNT and S-GNT (10 and 50 μM) were added. After 3 h and 24 h of exposure, the cells were trypsinized, resuspended in DMEM and centrifuged for 5 min. The cell suspension was resuspended in annexin V-PE (AV) and 7-amino-actinomycin-D (7-AAD)-labeled and incubated for 30 min. The data were collected and analyzed using a Guava easyCyte™ flow cytometer and Guava software (Millipore, USA). Three cell populations were detected: viable cells (AV −/7-AAD −), early apoptotic cells (AV +/7-AAD −), and late-stage apoptotic and dead cells (AV +/7-AAD +). For each sample examined, 5000 events were analyzed in three experiments.

2.7. Hoechst 33342 staining assay

Hoechst 33342 is a DNA-specific dye. Hoechst 33342 staining was performed to visualize morphologic characteristics of apoptosis, including nuclear condensation and the formation of apoptotic bodies. The cells were seeded in 6-well plates at a density of 10^5 cells/well. After 24 h of incubation, R-GNT and S-GNT (10 and 50 μM) were added. After 24 h and 48 h of exposure, the cells were stained with Hoechst 33342 (5 μg/mL) for 30 min at room temperature and observed immediately using a FLoid® Cell Imaging Station (magnification of 460×, blue filter, 390/40 nm excitation and 446/33 nm emission — Life Technologies, USA).

2.8. Single-cell gel electrophoresis assay (comet assay)

The alkaline comet assay was performed to investigate the genotoxic potential of goniothalamin according to the protocol of Tice et al. (2000) with some modification. The cells were seeded in 6-well plates at a density of 10^5 cells/well. After 24 h of incubation, R-GNT and S-GNT (10 and 50 μM) were added. After 3 h of exposure, the cells were trypsinized, resuspended in DMEM and centrifuged for 5 min. Subsequently, 20 μL of the cell suspension was mixed with 120 μL of low-melting point agarose (0.5%) and deposited onto a slide pregelatinized with agarose (normal melting point, 1.5%), and then covered with a coverslip and left to solidify. The slides were subject to 1 h lysis (2.5 M sodium chloride, 100 mM EDTA, 10 mM tris(hydroxymethyl)aminomethane (Tris), pH 10; 1% Triton X-100, and 10% DMSO). Alkaline denaturation for DNA unwinding (20 min) and electrophoresis (300 mA, 25 V, 20 min) were performed in a high pH buffer solution (200 mM EDTA, 10 N sodium hydroxide, and pH > 13). After electrophoresis, the slides were neutralized (0.4 M Tris and pH 7.5), dehydrated with ethanol, stained with 100 μL of 0.002 mg/mL ethidium bromide solution and scored using a fluorescence microscope equipped with a 420–490-nm UV excitation filter and a 520-nm barrier filter (Leica). The comets were classified by visual scoring into four categories based on the length of DNA migration (Collins et al., 2008): class 0, undamaged cells and nucleoids without tails; class 1, cells with damage and a tail smaller than the diameter of the nucleoid; class 2, cells with damage and a tail twice the diameter of the nucleoid; and class 3, cells with damage and a tail greater than twice the diameter of the nucleoid. The damage index (DI) was calculated as follows: $DI = N1 + (2 \times N2) + (3 \times N3)$, where N1, N2, and N3 represent the numbers of cells of damage levels 1, 2, and 3, respectively. For each sample examined, 100 cells were analyzed in three experiments. The cell viability analysis was conducted using the trypan blue stain exclusion method, and only treatments with an index greater than 80% were considered.

2.9. RT-qPCR

Cells were seeded in 6-well plates at a density of 10^5 cells/well. After 24 h of incubation, R-GNT (50 μM) was added and remained in culture for 12 h. After the treatment, total RNA was isolated using the RNeasy mini kit (Qiagen, USA) according to the manufacturer's recommendations. The RNA integrity was tested by agarose gel (1%) electrophoresis, and the concentration and purity (A260/A280) were quantified on a NanoDrop® 2000 (Thermo Fisher Scientific, USA). Isolated RNA was stored at −80 °C until processing. cDNA synthesis was performed using reverse transcriptase M-MLV (Invitrogen Life Technologies, USA) and total RNA using oligo (dT) primers (Invitrogen Life Technologies, USA) according to the protocol of the enzyme. Each RT-qPCR reaction was performed in a final volume of 11 μL containing 5 μL of cDNA, 5 μL of SsoAdvanced™ SYBR® Green Supermix (Bio-rad Laboratories, USA) and 1 μL of oligonucleotides. Quantitative PCR measurement reactions were performed using the real-time detection system CFX96 TOUCH™ (Bio-rad Laboratories, USA) and the following conditions: 50 °C for 2 min, 95 °C for 2:15 min, 60 °C for 15 s, and 72 °C for 30 s; 40 cycles. The melting point analysis was performed at the end of the reaction at a temperature of 55 °C to 95 °C every 0.5 °C for 5 s. The relative expression of each target gene was calculated using the average value of the CT between the target gene and the reference genes glyceraldehyde 3-phosphate dehydrogenase (*GAPDH*) and ribosomal protein L13a (*RPL13A*) (Table 1). The reference genes were selected according to the stability of gene expression among groups.

2.10. Statistical analysis

Data are presented as averages ± standard deviations of the three independent experiments. Differences were considered significant for P values less than 0.05. The cell viability, cell cycle, apoptosis and comet assay data were analyzed by analysis of variance (ANOVA) followed by Dunnett's post-hoc test. The IC50 values were calculated by non-linear regression (variable slope). RT-qPCR data were normalized and analyzed according to Pfaffl and Dempfle (2002) using REST 2009 software (Pair Wise Fixed Reallocation Randomisation Test©). To filter out unreliable data and to identify genes with significantly different expression, a standard 2-fold change in expression was used as the cut-off point. The real-time PCR efficiencies were estimated by LinRegPCR software.

3. Results

3.1. GNT reduces viability and cell growth

The MTT and Real-Time Cell Analyzer (RTCA) assays revealed that both R and S-GNT reduced the cell viability and growth of MCF-7 cells

Table 1
Sequences of primers used in RT-qPCR.

Symbol	Oligonucleotide		Ref. seq ID
CCNB1	*Forward*	AGA GCA TCT AAG ATT GGA GAG	Sigma
	Reverse	CCA TGT CAT AGT CCA ACA TAG	
CCNB2	*Forward*	ATT TTT ACA GGT TCA GCC AG	Sigma
	Reverse	ATC TCC TCA TAC TTG GAA GC	
CCND1	*Forward*	GCC TCT AAG ATG AAG GAG AC	Sigma
	Reverse	CCA TTT GCA GCA GCT C	
CCNE1	*Forward*	GAC TTA CAT GAA GTG CTA CTG	Sigma
	Reverse	GAC GAG AAA TGA TAC AAG GC	
CDK1	*Forward*	ATG AGG TAG TAA CAC TCT GG	Sigma
	Reverse	CCT ATA CTC CAA ATG TCA ACT G	
CDK2	*Forward*	GAG ACC TTA AAC CTC AGA ATC	Sigma
	Reverse	TGG AAT AAT ATT TGC AGC CC	
CDK4	*Forward*	GAA CAT TCT GGT GAC AAG TG	Sigma
	Reverse	CAA AGA TAC AGC CAA CAC TC	
CDK6	*Forward*	GGA TAT GAT GTT TCA GCT TCT C	Sigma
	Reverse	TCT GGA AAC TAT AGA TGC GG	
CDK7	*Forward*	CTA GGA TGT ATG GTG TAG GTG	Sigma
	Reverse	AAG GAA CCC TTA GAA GTA ACT C	
CDKN1A	*Forward*	CAG CAT GAC AGA TTT CTA CC	Sigma
	Reverse	CAG GGT ATG TAC ATG AGG AG	
CDKN1B	*Forward*	AAC CGA CGA TTC TTC TAC TC	Sigma
	Reverse	TGT TTA CGT TTG ACG TCT TC	
CDKN1C	*Forward*	CAA GTC TGT TAA AAT GGT TCC	Sigma
	Reverse	TTT TTG CAG CAT TTT TCG G	
CASP9	*Forward*	CTC TAC TTT CCC AGG TTT	Sigma
	Reverse	TTT CAC CGA AAC AGC ATT	
CASP8	*Forward*	GCA AAA GCA CGG GAG AAA GT	Castaneda and Rosin-Steiner (2006)
	Reverse	TGC ATC CAA GTG TGT TCC ATT C	
GADD45a	*Forward*	TCA GCG CAC GAT CAC TGT C	Constructed
	Reverse	CCA GCA GGC ACA ACA CCA C	
GAPDH	*Forward*	GAA GGT GAA GGT CGG AGT C	Sugaya et al. (2005) with modifications
	Reverse	GGA AGA TGG TGA TGG GAT TT	
RPL13A	*Forward*	CCT GGA GGA GAA GAG GAA AGA GA	Brandimarto (2009)
	Reverse	TTG AGG ACC TCT GTG TAT TTG TCA A	

and HB4a in a dose- and time-dependent manner (Figs. 2 and 3). Both the MTT assay and cell growth kinetics analysis revealed that the natural enantiomer R-GNT is more effective in reducing the cell viability and cell growth than the enantiomer S-GNT.

Assessment of HB4a and MCF-7 cell viability was performed by MTT assay (Fig. 2). There was a significant reduction in the cell viability of HB4a cells at all tested concentrations of R-GNT after 24 h (Fig. 2A) and 48 h (Fig. 2B). MCF-7 cells also exhibited reduced viability after 24 h (Fig. 2A) and 48 h (Fig. 2B) of exposure at all concentrations of R-GNT tested, except at 1 μM. S-GNT reduced HB4a cell viability after exposure at all concentrations, except at 1 and 30 μM after 24 h (Fig. 2C) and 1 μM after 48 h (Fig. 2D). MCF-7 cells exhibited reduced cell viability after 24 h of exposure at all concentrations of S-GNT (Fig. 2C). After 48 h, 1 and 10 μM of S-GNT did not reduce MCF-7 cell viability (Fig. 2D).

The half-maximal inhibitory concentration (IC50) defined by the MTT assay of R-GNT after 48 h was 11.7 μM ($R^2 > 0.9$) for HB4a and 52.12 μM for MCF-7 ($R^2 > 0.9$), and the IC50 of S-GNT was 50.86 μM ($R^2 > 0.8$) for HB4a and >100 μM for MCF-7 cells ($R^2 = 0.8$). Therefore, for subsequent experiments, R and S-GNT were used at concentrations of 10 μM and 50 μM.

The assessment of real-time cell growth kinetics performed using the xCELLigence Real Time Cell Analyzer (RTCA) equipment (Fig. 3) revealed that the R-GNT (50 μM and 100 μM) caused a great reduction in the cell index as early as 3 h after treatment of HB4a (Fig. 3A) and MCF-7 cells (Fig. 3D). The HB4a cells treated with R-GNT (1 μM) showed a cell growth similar to the control group. Upon 10 μM, there was a reduction in normalized cell index according to the concentration of R-GNT (Fig. 3A). Also the S-GNT showed a decrease in cell growth compared to the control group from the concentration of 20 μM (Fig. 3B). MCF-7 cells presented a dose-dependent cell growth inhibition when treated with R-GNT from the concentration of 20 μM (Fig. 3D). Already only the highest concentration (100 μM) of S-GNT reduced the MCF-7 cell growth (Fig. 3E). Consistent to the cell growth curves, the photomicrographs showed that there was a reduction in cell density and morphological changes such as rounding and shrinkage of HB4a (R-GNT: 10 and 50 μM; S-GNT: 50 μM) and of MCF-7 cells (R-GNT: 50 μM) (Fig. 3C and F).

3.2. Goniothalamin induces cell cycle arrest

To investigate the mechanisms by which goniothalamin inhibits cell growth, cell cycle (G1, S, G2, and sub-G1) analysis by flow cytometry was performed after 3 and 24 h of treatment with R and S-GNT (10 and 50 μM).

There was a slight reduction in the number of HB4a cells in the G0/G1 cell cycle phase ($p < 0.05$) and a small, though not significant, increase in the number of cells in the G2/M phase after 3 h of treatment with R-GNT (10 and 50 μM) and S-GNT (50 μM) (Fig. 4A and B). After 24 h of treatment with 50 μM R-GNT, we observed an increase in the G2/M phase cell population (control: 35.15%; 50 μM R-GNT: 48.30%) ($p < 0.001$) and a decrease in the number of cells in the G0/G1 phase (control: 46.56%; 50 μM R-GNT: 24.22%) ($p < 0.001$) (Fig. 4A and C).

The analysis of the cell cycle distribution of MCF-7 cells demonstrates that after 3 h of treatment with R-GNT (10 μM) and S-GNT (10 μM) there was a slight decrease in the number of cells in the G0/G1 phase ($p < 0.05$) (Fig. 4D and E). After 24 h of treatment (Fig. 4D and Fig. 4F), we observed a significant increase in the number of MCF-7 cells in the G0/G1 phase after treatment with R-GNT (10 μM) and S-GNT (10 and 50 μM) (Control: 44.10%; 10 μM R-GNT: 59.24%; 10 μM S-GNT: 54.51%; 50 μM of S-GNT: 57.63%) ($p < 0001$). This increase in the G0/G1 phase cell population was accompanied by a reduction in the number of S phase cells in the groups treated with 10 μM R-GNT

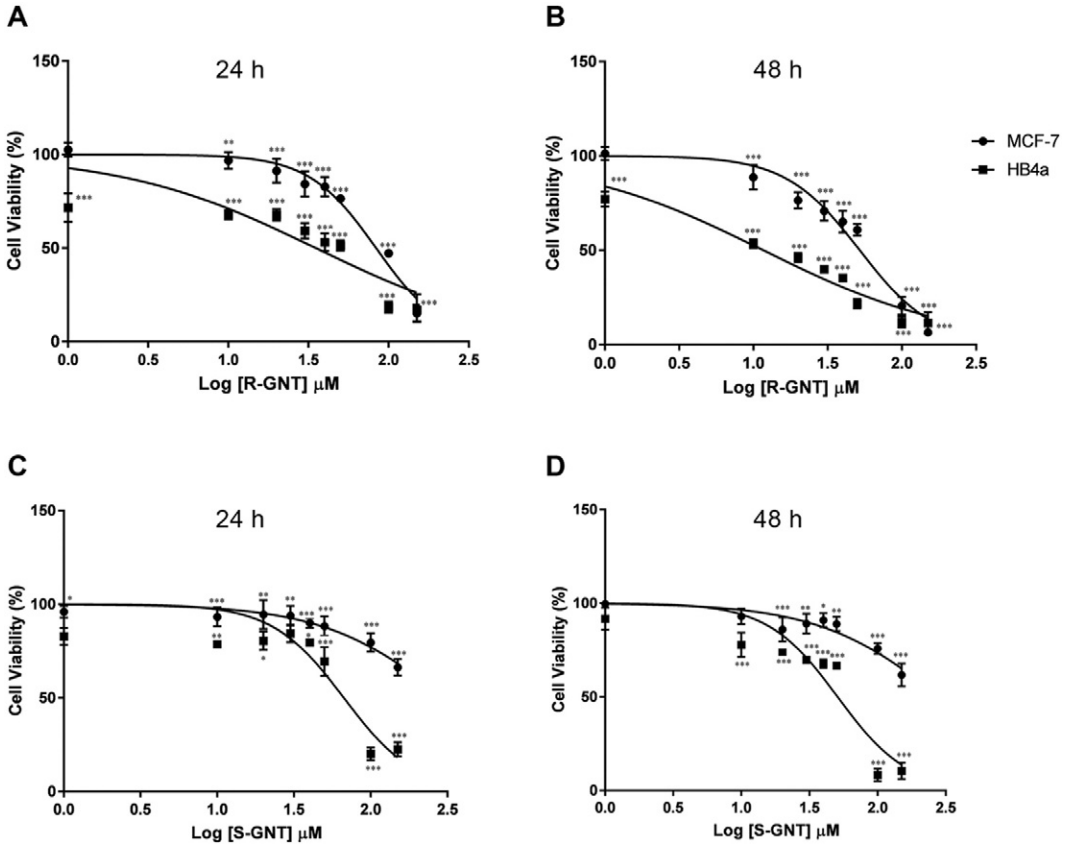

Fig. 2. Cell viability (%) of MCF-7 and HB4a breast cell lines after 24 and 48 h of incubation with 1–150 μM of R-GNT and S-GNT measured using the MTT assay. (A) Cell viability (%) after exposure to R-GNT for 24 h and (B) 48 h. (C) Cell viability (%) after exposure to S-GNT for 24 h and (D) 48 h. Results are presented as the mean ± SD of three independent experiments. * $p < 0.05$, ** $p < 0.01$, *** $p < 0.001$ relative to control using ANOVA followed by Dunnett.

($p < 0.001$) and 50 μM S-GNT ($p < 0.01$) (Control: 13.17%; 10 μM R-GNT: 1.67%; 50 S-GNT: 5.76). In the group treated with 10 μM S-GNT, the increase in the G0/G1 cell population was accompanied by a decrease in the number of G2/M cells (Control: 34.76%; 10 μM S-GNT: 25.85%) ($p < 0.001$). In addition, we observed a slight but not significant increase in the population of cells in the G2/M phase after treatment with 50 μM R-GNT (Control: 34.7%; 50 μM R-GNT: 40%) as well as a slight reduction in cell population in the S phase (Control: 13%; 50 μM R-GNT: 9.8%).

These results suggest that the treatment of HB4a cells with 50 μM R-GNT induced G2/M cell cycle arrest, whereas the treatment of MCF-7 cells with R-GNT (10 μM) and S-GNT (10 and 50 μM) induced cell cycle arrest in the G0/G1 phase.

3.3. Goniothalamin induces apoptosis

To investigate the mechanisms of goniothalamin cytotoxicity, the induction of apoptotic cell death was measured by annexin V-7AAD assay after 24 h of treatment with R- and S-GNT (10 and 50 μM) (Fig. 5). The treatment of HB4a cells with R-GNT (10 and 50 μM) and S-GNT (50 μM) caused a decrease in the number of viable cells (Control: 87.83%; 10 μM R-GNT: 81.13%; 50 μM R-GNT: 62.70%; 50 μM S-GNT: 81.10%) ($p < 0.001$) and an increase in cells in the early stage of apoptosis (Control: 7.67%; 10 μM R-GNT: 11.90%; 50 μM R-GNT: 17.57%; 50 μM S-GNT: 12.23%) ($p < 0.001$). Moreover, treatment with R-GNT (50 μM) caused an increase in the number of cells in the late stages of apoptosis (Control: 3.80%; 50 μM R-GNT: 19.30% — $p < 0.001$) (Fig. 5A and B).

The analysis of the MCF-7 cells demonstrates that there was a little decrease in the number of cells in late apoptosis (Control: 8.10%; 50 μM S-GNT: 4.87%) ($p < 0.01$). Treatment with 50 μM R-GNT induced a decrease in the number of viable cells (Control: 90.20%; 50 μM: 83.20%) ($p < 0.001$) and an increase in the number of cells in late-stage apoptosis (Control: 8.10%; 50 μM: 15.17%) ($p < 0.001$) (Fig. 5C and D).

The total proportion of apoptotic cells labeled with annexin V (AV+/7-AAD+ and AV+/7-AAD−) after treatment with 50 μM R-GNT was 36.87% for HB4a cells and 16.34% for MCF-7 cells. The Hoechst 33342 staining showed that the most of the HB4a (Fig. 5A) cells and MCF-7 cells (Fig. 5C) in the control group exhibited normal staining of chromatin and normal nuclear morphology, whereas there was an increase in the number of cells that exhibited strong fluorescence, chromatin condensation, and fragmented nuclei in the MCF-7 cells treated with R-GNT (50 μM) and in HB4a cells treated with R-GNT and S-GNT (10 and 50 μM).

3.4. Goniothalamin induces DNA damage

DNA damage can result in cell cycle arrest and cell death by apoptosis. To investigate the potential of goniothalamin to induce DNA damage in HB4a and MCF-7 cells, a Comet Assay was performed after 3 h of treatment with R-GNT and S-GNT (10 μM and 50 μM).). The analysis of the damage index (DI) showed that treatment of HB4a cells with R-GNT (50 μM) ($p < 0.01$) (Fig. 6A) and of MCF-7 cells with R-GNT (10 μM and 50 μM) and S-GNT (10 μM and 50 μM) resulted in induction of DNA damage ($p < 0.01$) (Fig. 6B). The S-GNT was not genotoxic to HB4a cells.

3.5. (R)-goniothalamin changes the expression of cell cycle control genes

R-GNT dramatically changed the cell cycle dynamic and induced apoptosis in both mammary cell lines examined. Thus, to analyze the effects of R-GNT in the regulation of genes involved in the cell cycle and apoptosis pathway, cells were treated with 50 μM R-GNT for 12 h,

followed by measurement of mRNA levels by RT-qPCR. The analysis of HB4a cells (Fig. 7A) revealed that the mRNA levels of cyclins (*CCNB1*: 5.2-fold-change and *CCNB2*: 5.2-fold-change) and CDKs (*CDK1*: 2.3-fold-change and *CDK4*: 2.82-fold-change) were downregulated. The mRNA levels of the cyclin-dependent kinase inhibitor *CDKN1A* was upregulated (14-fold-change). In MCF-7 cells (Fig. 7B), the mRNA levels of cyclins (*CCND1*: 2.79-fold-change; *CCNB1*: 4.5-fold-change, *CCNB2*: 6.7-fold-change) and CDKs (*CDK1*: 8.3-fold-change, *CDK2*: 4.3-fold-change and *CDK4*: 2-fold-change) were downregulated, whereas the levels of the cyclin-dependent kinase inhibitor *CDKN1A* (16.6-fold-

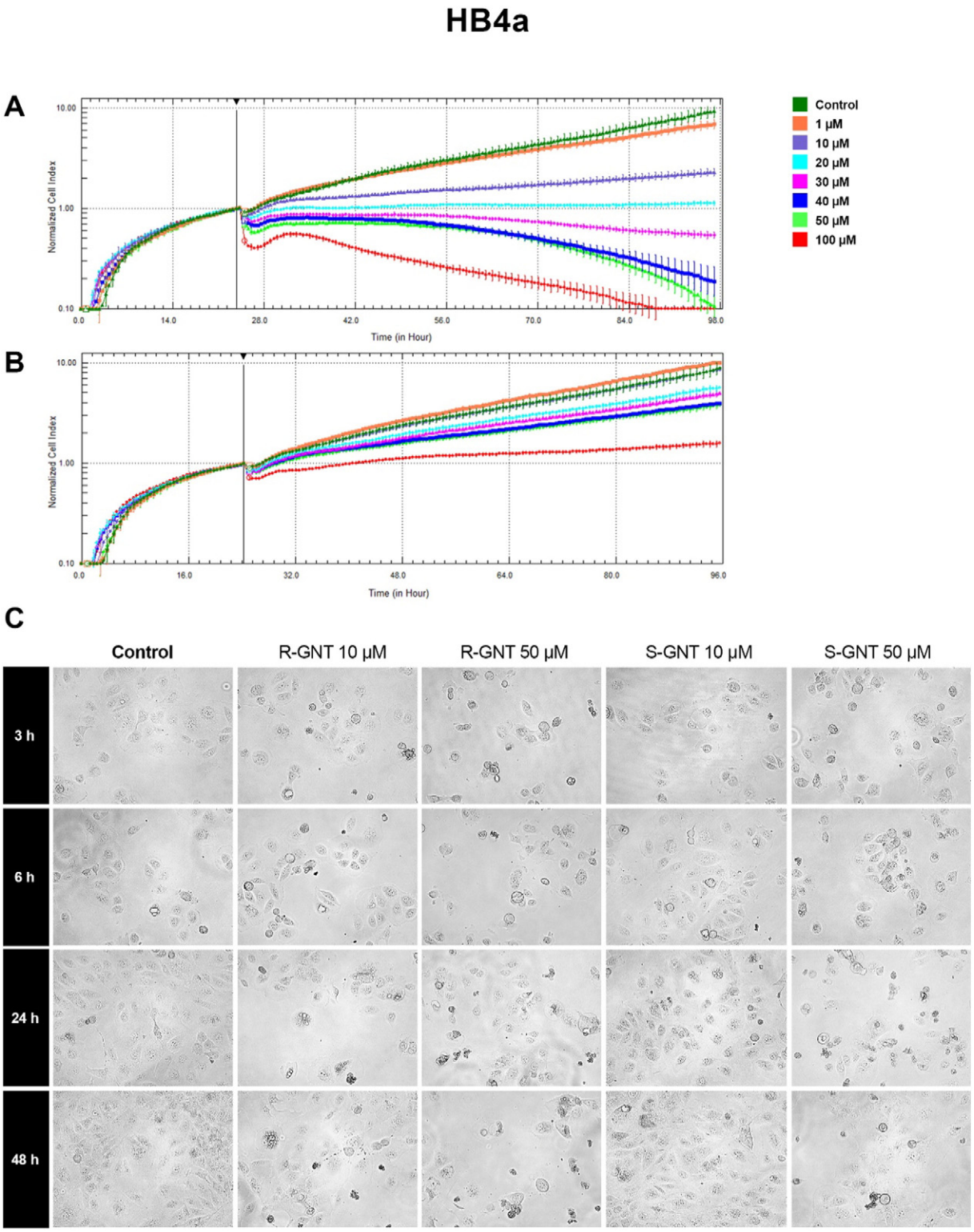

Fig. 3. Real-time monitoring of HB4a and MCF-7 cells obtained using the xCELLigence system demonstrating the kinetics of cell growth after exposure to R-GNT and S-GNT (1, 10, 20, 30, 40, 50 and 100 µM). (A) Growth curves of HB4a cells exposed to R-GNT and (B) S-GNT. (C) Photomicrograph of HB4a cells after treatment with R-GNT and S-GNT (10 µM and 50 µM) for 3, 6, 24 and 48 h. (D) Growth curves of MCF-7 cells exposed to R-GNT and (E) S-GNT. (F) Photomicrograph of MCF-7 cells after treatment with R-GNT and S-GNT (10 µM and 50 µM) for 3, 6, 24 and 48 h (460× magnification). The results are presented as the means of three replicates with standard error bars.

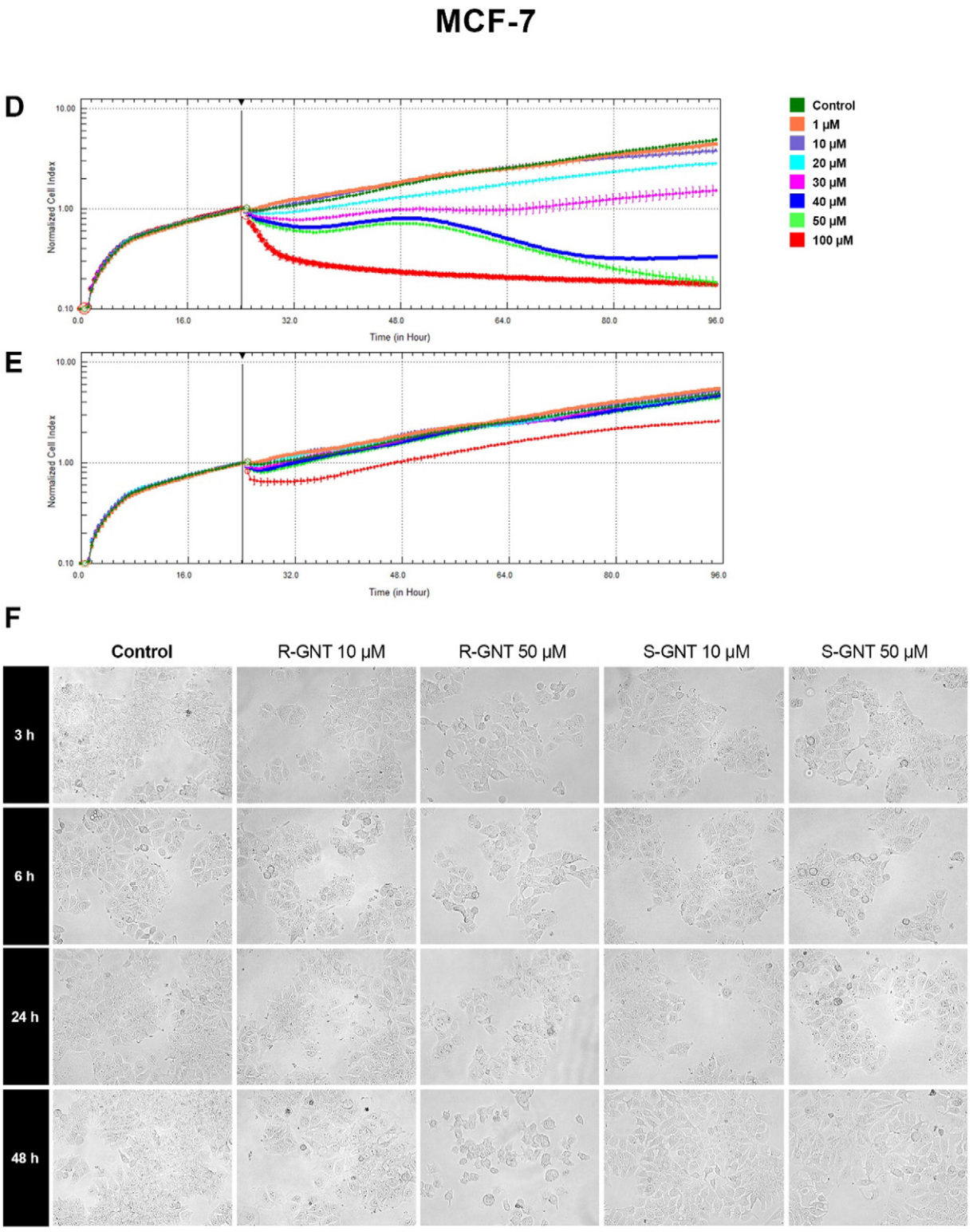

Fig. 3 (*continued*).

change) and *CDKN1C* (3.5-fold-change) were upregulated. *CDKN1A* was the most responsive gene after treatment with R-GNT, with a greater than sixteen- and fourteen-fold increase in expression in MCF-7 and HB4a cells, respectively. The mRNA levels of genes that encode caspase 8 (*CASP8*) and caspase 9 (*CASP9*) were unchanged (Fig. 8).

The mRNA levels of *GADD45a* was investigated by RT-qPCR after 3 h and 12 h of exposure to genotoxic concentrations of R-GNT (50 μM) (Fig. 9). The mRNA levels of the *GADD45a* gene were upregulated after 12 h of exposure to R-GNT in both cell lines (HB4a: 4.74-fold-change; MCF-7: 9-fold-change).

4. Discussion

Evidence obtained from *in vitro* (Alabsi et al., 2012; de Fatima et al., 2008) and *in vivo* experiments (Vendramini-Costa et al., 2010) indicates that goniothalamin might have therapeutic potential for the treatment

of cancer. In this study, we determined that goniothalamin exhibits dose- and time-dependent antiproliferative activity against HB4a and MCF-7 cells. Both cell viability and cell growth kinetic analysis revealed that the natural enantiomer R-GNT was more effective than the synthetic enantiomer S-GNT. The antiproliferative activity of goniothalamin against the MCF-7 and HB4a cells appeared to be the result of cell cycle arrest and the induction of cell death by apoptosis, probably in response to the induction of DNA damage. This is the first study that demonstrated the influence of GNT in the regulation of the expression of genes involved in cell cycle control.

Among all of the bioactive properties described, the antiproliferative activity of goniothalamin against cancer cells is most notable. Moreover, some authors have suggested a possible selectivity of goniothalamin against tumor cell lines with limited activity against normal cells, which has attracted interest in this molecule in the last two decades (Pihie et al., 1998; Tian et al., 2006; Wattanapiromsakul et al.,

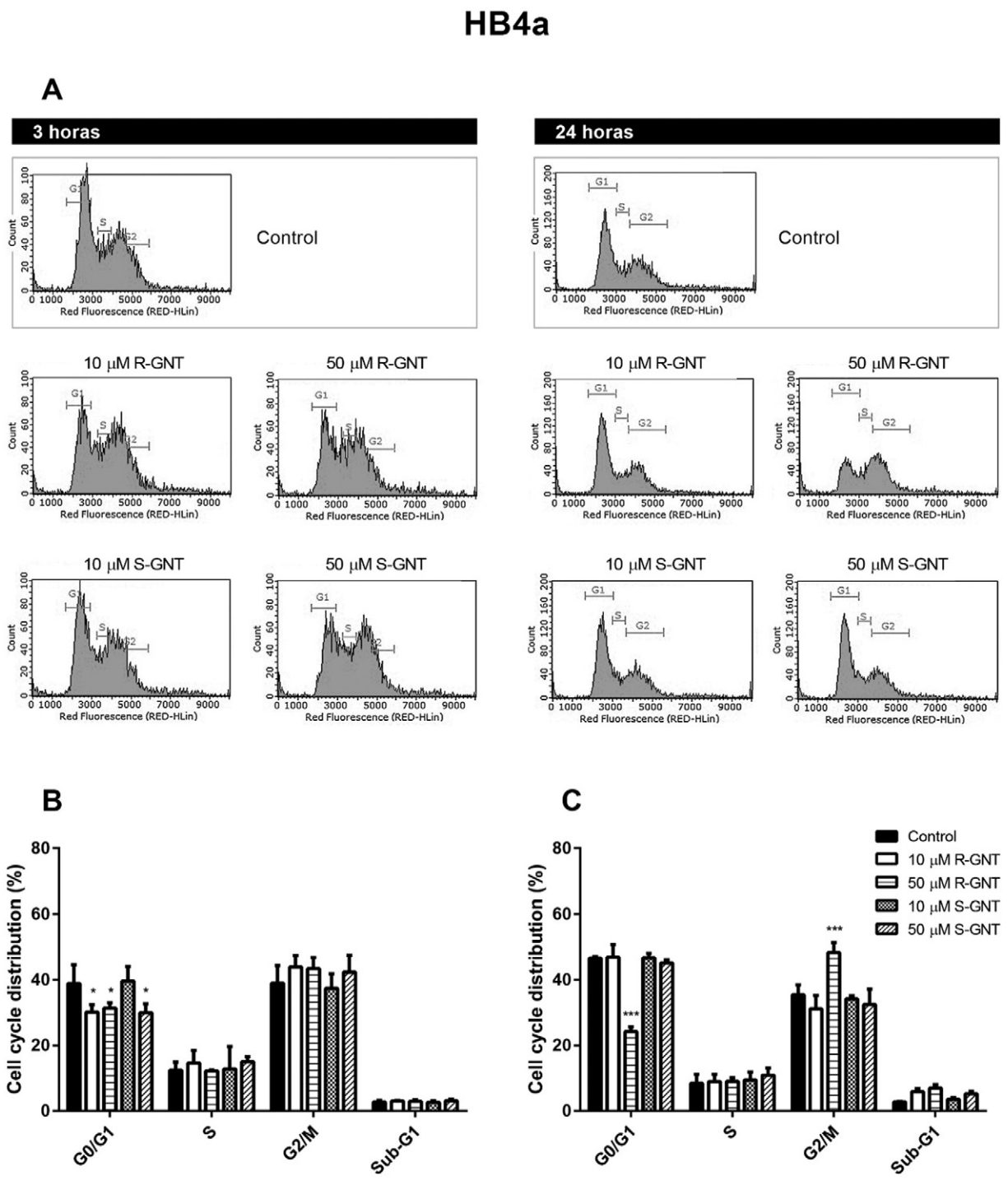

Fig. 4. Cell cycle analysis (G0/G1, S, G2/M and subG1) of HB4a and MCF-7 cells after exposure to R and S-GNT (10 μM and 50 μM) by flow cytometry using propidium iodide labeling. (A) Representative histograms indicate the number of cells (vertical axis) vs. DNA content (horizontal axis) after 3 and 24 h of treatment of HB4a cells with R and S-GNT (10 μM and 50 μM). (B) HB4a cell cycle distribution after 3 h of exposure to R and S-GNT (10 μM and 50 μM) and (C) after 24 h. (D) Representative histograms depict the number of cells (vertical axis) vs. DNA content (horizontal axis) after 3 and 24 h of treatment of MCF-7 cells with R and S-GNT (10 μM and 50 μM). (E) MCF-7 cell cycle distribution after 3 h of exposure to R and S-GNT (10 μM and 50 μM) and (F) after 24 h. Results are presented as the mean ± SD of three independent experiments. * $p < 0.05$, ** $p < 0.01$, *** $p < 0.001$ relative to control using ANOVA followed by Dunnett.

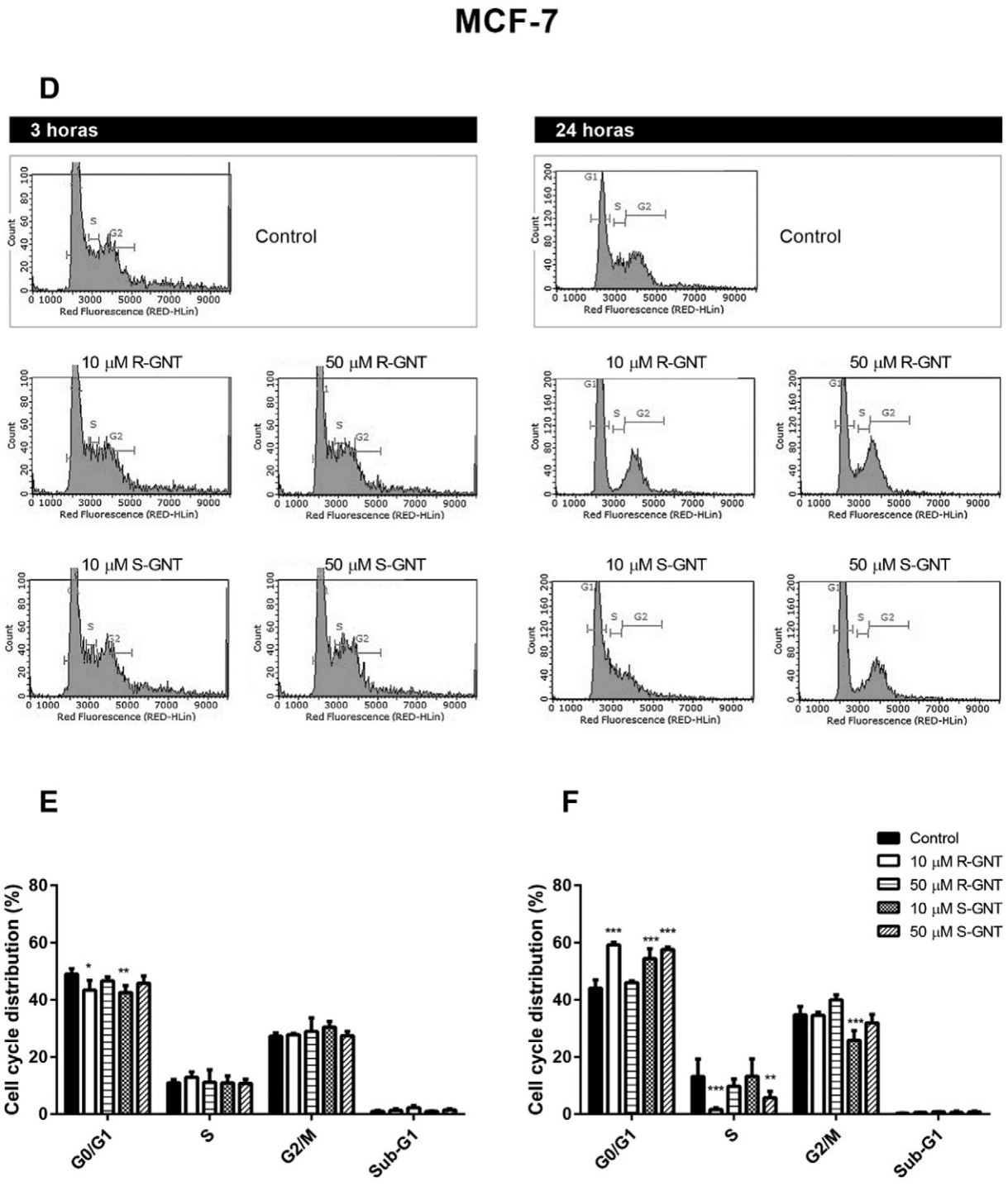

Fig. 4 (*continued*).

2005). In the present study, we observed a potent cytotoxic and antiproliferative effect of goniothalamin against breast cell lines at low concentrations in a dose- and time-dependent manner. However, there was no selective cytotoxicity for MCF-7 tumor cells relative HB4a non-tumor cells.

The analysis of real-time cell growth allows us to verify the effects of a given compound at several points of time, permitting dynamic monitoring of the effects of a compound on cell growth (Abassi et al., 2009). Cell growth inhibition after exposure to R-GNT began within the first 3 h, demonstrating an early cellular response to treatment. In both the MTT assay and RTCA analysis, the natural enantiomer R-GNT proved more effective against both cell lines relative to the synthetic enantiomer S-GNT. Although both enantiomeric forms exhibit the same chemical and physical properties, their biological activities differ considerably, likely due to the specific interactions of enantiomers with biological receptors (Tucker, 2000).

Cell index (CI) variations reflect alterations in cellular biological status, including the number of cells, cell viability, morphology and adhesion. The cell viability determined by MTT assay can be defined as the number of healthy cells; however, it is not possible to distinguish whether the cells are actively dividing or are quiescent. Therefore, we investigated the effects of GNT in the range close to the IC50 of R-GNT values for HB4a (10 μM) and MCF-7 (50 μM) on the ability to induce cell death by apoptosis and to cause cell cycle arrest. Consistent with

the observation of a decrease in the cell index, we observed that goniothalamin was able to induce DNA damage, cell cycle arrest and apoptosis.

The cellular DNA damage response (DDR) detects DNA lesions and initiates DNA damage checkpoints. DNA damage checkpoints occur throughout the cell cycle, and the cells may transiently arrest in the G1/S or G2/M transitions or may permanently arrest (senescence) and activate DNA repair mechanisms in response to genotoxic insults. If the DNA damage is not amenable to repair, the cells may undergo death by apoptosis (Cheung-Ong et al., 2013). R-GNT was able to induce

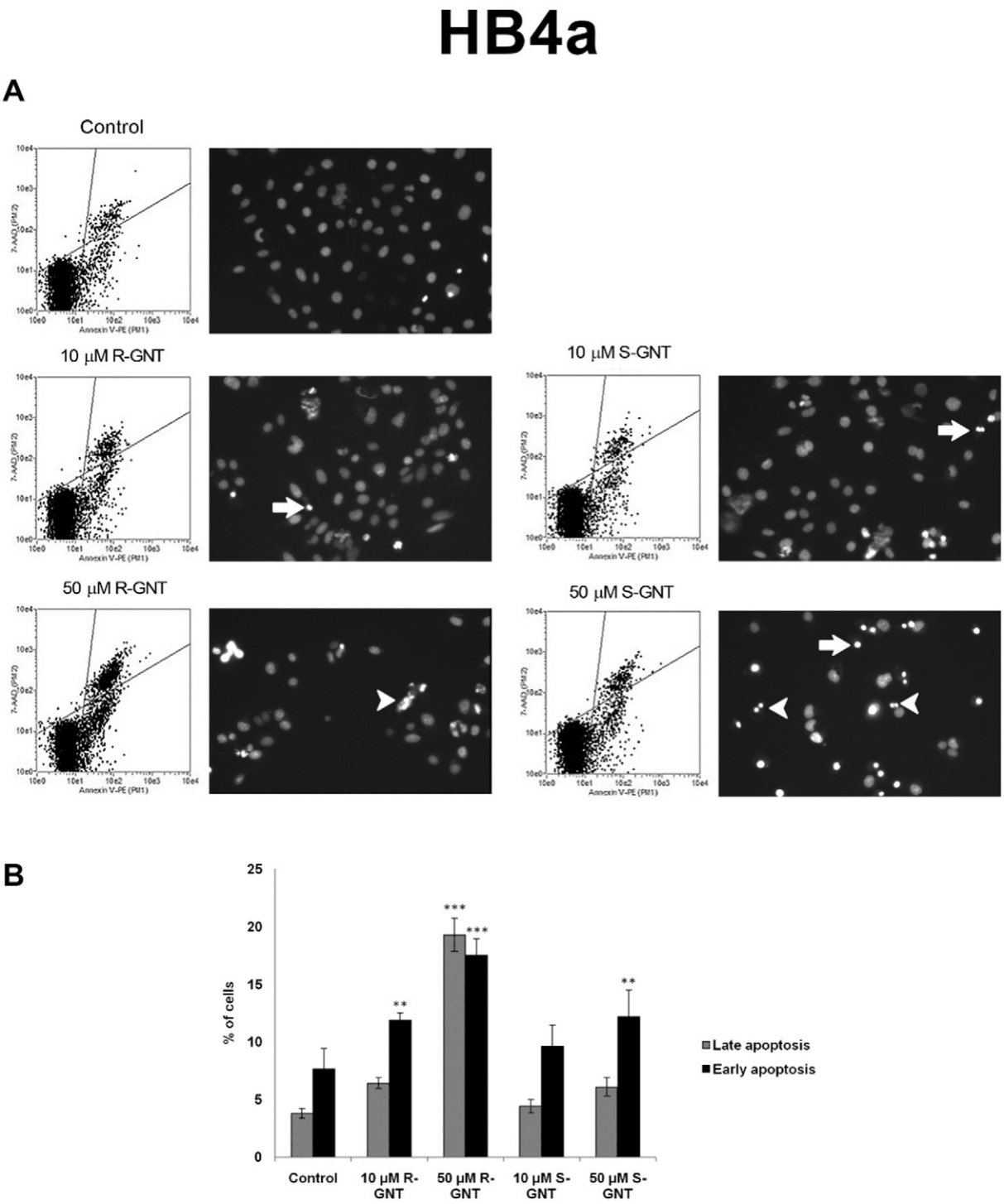

Fig. 5. Effects of R-GNT and S-GNT (10 μM and 50 μM) on apoptosis induction. The apoptosis analysis was performed by flow cytometry using Annexin V-PE (AV) and 7-amino-actinomycin D (7-AAD), and the events were classified into three cell populations: viable cells (AV−/7-AAD−), early apoptotic cells (AV+/7-AAD−), and late stage apoptotic and dead cells (AV+/7-AAD+). (A) Representative graphs of quantification of annexin V (AV) and 7-amino-actinomycin D (7-AAD) staining and photomicrographs showing morphology and the staining with Hoechst 33342 of HB4a cells. (B) Percentage of HB4a cells in early and late apoptosis after 24 h of treatment with R-GNT and S-GNT (10 μM and 50 μM). (C) Representative graphs of quantification of annexin V (AV) and 7-amino-actinomycin D (7-AAD) staining and photomicrographs showing morphology and the staining with Hoechst 33342 of MCF-7 cells. (D) Percentage of MCF-7 cells in early and late apoptosis after 24 h of treatment with R-GNT and S-GNT (10 μM and 50 μM). Results are mean ± SD of three independent experiments. * $p < 0.05$, ** $p < 0.01$, *** $p < 0.001$ compared to control using ANOVA followed by Dunnett. Arrow indicates cells with condensed chromatin and arrowhead indicates the apoptotic bodies (magnification = 460×).

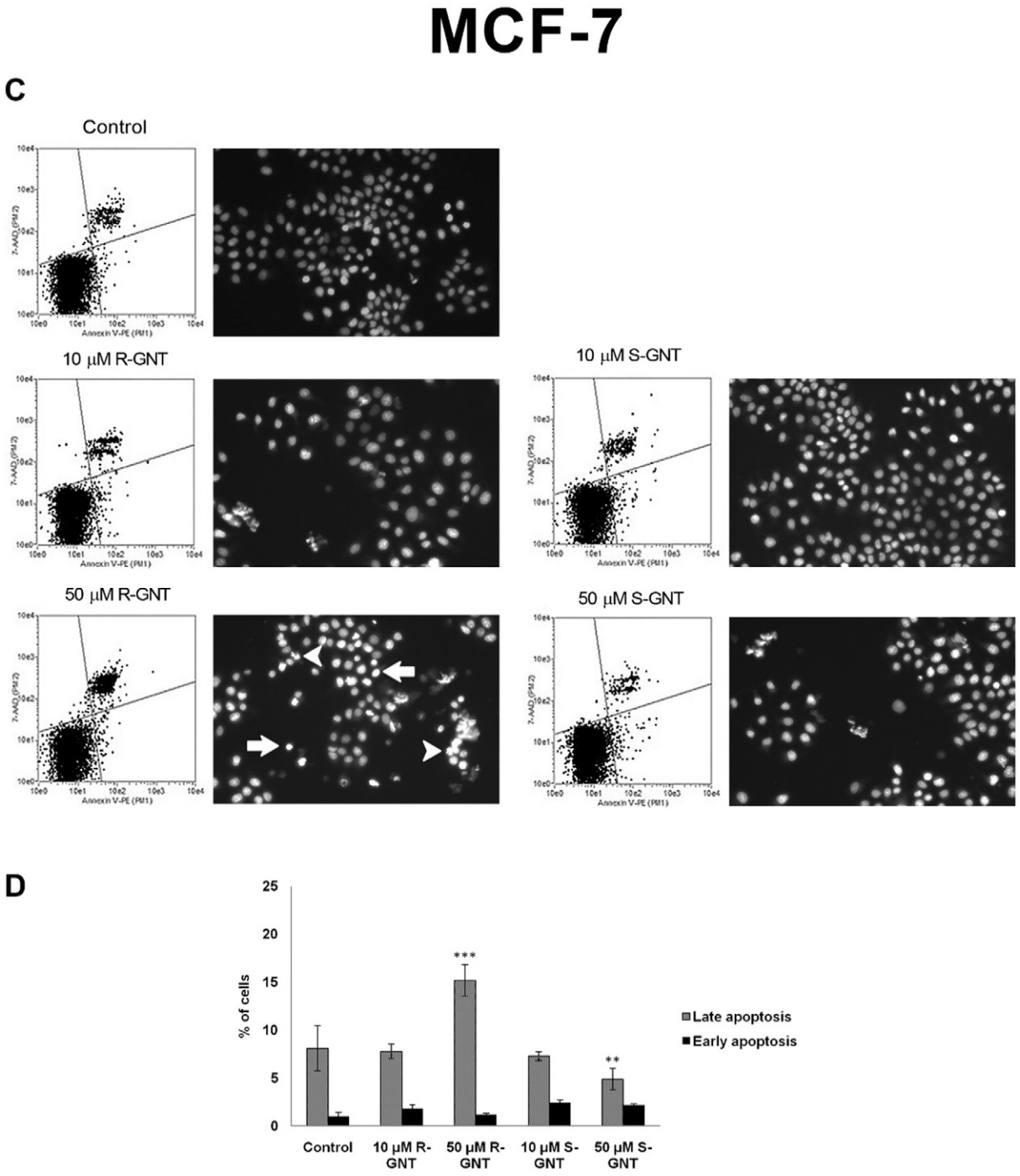

Fig. 5 (*continued*).

genotoxicity in HB4a and MCF-7 cells. S-GNT, in turn, was genotoxic only for the tumor cell line MCF-7. These results are consistent with previous reports that attribute the cytotoxic effect of goniothalamin to its genotoxicity (Inayat-Hussain et al., 2009; Kuo et al., 2011; Rajab et al., 2005). In addition, the gene *GADD45a*, which is regulated in response to DNA damage, was upregulated after R-GNT exposure. Accumulating evidence suggests that the overexpression of the growth arrest and DNA damage (Gadd) 45a gene (*GADD45a*) suppress cell proliferation through cell cycle arrest and apoptosis induction (Tamura et al., 2012). Numerous studies have found a correlation between the upregulation of GADD45a and G2/M cell cycle arrest (Jin et al., 2002; Li et al., 2009; Wang et al., 1999). This response occurs because the Gadd45α protein strongly inhibits the kinase activity of the complex CDK1/Cyclin B1, which is responsible for transitioning the G2 cell to mitosis (Jin et al., 2000).

After DNA damage, p53 protein is activated and upregulates target genes that control the cellular response, such as *CDKN1A*, a gene that encodes the p21 protein. Our gene expression analysis revealed that the mRNA levels of *CDKN1A* were markedly up-regulated after R-GNT treatment in both cell lines. *CDKN1C*, which also belongs to the CIP/KIP cyclin-kinase inhibitor family, was also up-regulated in MCF-7 cells after treatment with R-GNT. It is well established that induction of the p21 response associated with DNA damage causes cell cycle arrest in the G1 and G2 phases (Abbas and Dutta, 2009).

R-GNT (50 μM) induced cell cycle arrest in the G2/M phase in HB4a cells. In MCF-7 cells, we observed G1 arrest when the cells were exposed

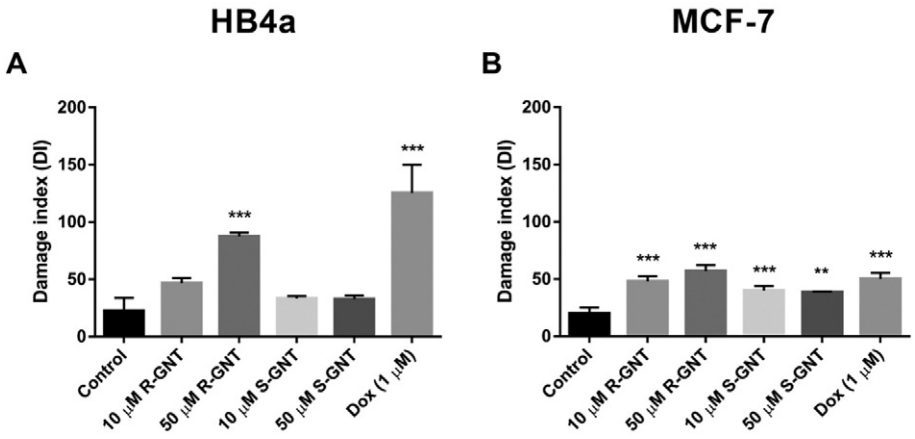

Fig. 6. Evaluation of the damage index (DI) after 3 h of exposure of HB4a and MCF-7 cells to R-GNT and S-GNT (10 μM and 50 μM) measured using the Comet Assay. (A) Damage Index (DI) in HB4a and (B) MCF-7 cells. Data are presented as the mean ± SD of three independent experiments. * $p < 0.05$, ** $p < 0.01$, *** $p < 0.001$ relative to the control group using ANOVA followed by Dunnett.

to R-GNT (10 μM) and to S-GNT (10 μM and 50 μM). Moreover, the treatment of MCF-7 cells with a higher concentration of R-GNT (50 μM) caused a slight increase in the population of cells in the G2/M phase. Other authors has been attributed the antiproliferative activity of goniothalamin to cell cycle arrest at the G0/G1 (Barcelos et al., 2014), G2/M (Chen et al., 2005; Tian et al., 2006) and S phases (Alabsi et al., 2012). Exposure of HepG2 cells and HepG2-R to GNT (15 μM) caused G2/M cell cycle arrest and increased the sub-G1 population (Tian et al., 2006). The treatment of MDA-MB-231 cells with GNT (30 μM) also led to cell cycle arrest at the G2/M phase with a concomitant reduction in G1 (Chen et al., 2005). On the other hand, Barcelos et al. (2014) suggested that PANC-1 cells exposed to GNT exhibit G0/G1 cell cycle arrest.

Analysis of the expression levels of cell cycle machinery components by RT-qPCR revealed the downregulation of some cyclins and CDKs. The mRNA levels of *CCND1* and *CDK4* were downregulated in MCF-7 cells, but only *CDK4* was downregulated in non-tumoral HB4a cells. The downregulation of *CCND1*, a gene that encodes cyclin D1, observed in MCF-7 cells is consistent with a previous study reporting that the exposure of PANC-1 cells to GNT led to a decrease in the cyclin D1 protein levels and in the phosphorylation of Rb protein (Barcelos et al., 2014). The overexpression of cyclin D1 is a feature of breast cancer, occurring in 50% of cases, and MCF-7 breast cancer cells express high levels of cyclin D1 (Zhou et al., 1997). Thus, cyclin D is partially responsible for the excessive proliferation of cancer cells in many human cancers and is therefore a good target for the development of anticancer drugs (Musgrove et al., 2011). Moreover, the cyclin E/CDK2 complex is required for cells to transition from G1 to S. This complex contributes to the maintenance of hyperphosphorylated Rb and the positive feedback stimulating the accumulation of E2F. The association of CDK2 with cyclin A also contributes to DNA replication (Malumbres and Barbacid, 2009). Although there were no changes in the mRNA levels of cyclin E1, the levels of CDK2 were drastically reduced in MCF-7 cells.

The G2–M cell cycle phase transition is regulated by CDK1 in association with cyclins A, B1 and B2. These complexes phosphorylate cytoskeletal proteins and mitotic spindle components (Nigg, 2001). In both cells, we observed the downregulation of genes that encode cyclins B1 and B2 as well as CDK1. Therefore, the reduced expression of cyclin D1 and CDK4 mRNA in addition to the downregulation of CDK2 in MCF-7 cells, both positive regulators of the G1-S transition, could be related to G1 cell cycle arrest. However, R-GNT induced G0/G1 cell cycle arrest in MCF-7 cells only at the lower tested concentration of R-GNT (10 μM). On the other hand, the downregulation of *CCNB1*, *CCNB2* and *CDK1* in both cell lines may contribute to the evident G2/M cell cycle

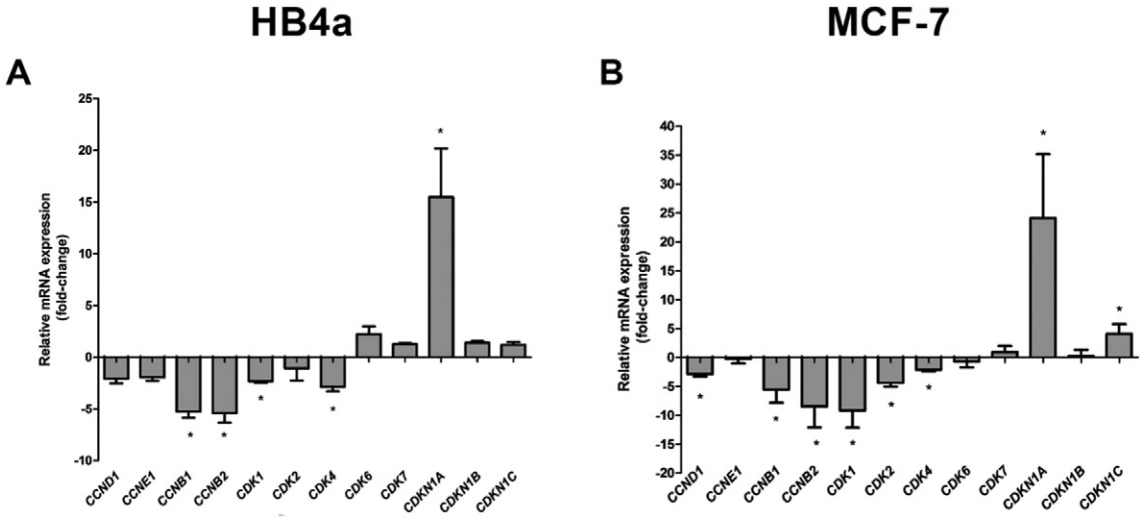

Fig. 7. RT-qPCR analysis of genes involved in cell cycle regulation. Graphs shown the relative gene expression (fold-change) of cyclins, CDKs and CKIs genes in (A) HB4a and (B) MCF-7 cells after 12 h of exposure to R-GNT 50 μM. The relative expression of each target gene was normalized with the reference genes Glyceraldehyde 3-phosphate dehydrogenase (GAPDH) and ribosomal protein L13a (RPL13A). Data are expressed as fold changes relative to control group in three independent experiments (mean ± SEM). Statistical differences compared to control are indicated by * (REST 2009 software ®).

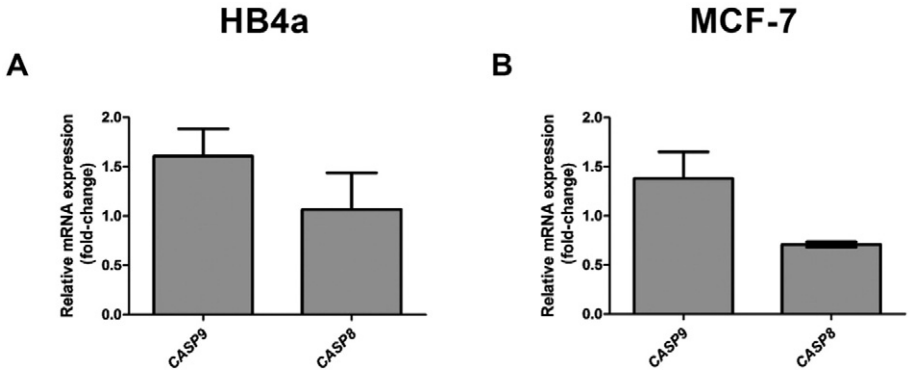

Fig. 8. RT-qPCR analysis of genes involved apoptosis pathway. Graphs shown the relative gene expression (fold-change) of CASP9 and CASP8 in (A) HB4a and (B) MCF-7 cells after 12 h of exposure to R-GNT 50 μM. The relative expression of each target gene was normalized with the reference genes glyceraldehyde 3-phosphate dehydrogenase (GAPDH). Data are expressed as fold changes relative to control group in three independent experiments (mean ± SEM). Statistical differences compared to Control are indicated by * (REST 2009 software ®).

arrest after R-GNT treatment in HB4a cells and to the slight increase in the population of cells in the G2/M phase after treatment of MCF-7 cells with 50 μM R-GNT. This finding suggests that the relative contribution of G1 arrest or G2/M arrest may vary according to the cell line, treatment time and dose. Moreover, the *CDKN1A* upregulation might contribute to downregulation of cyclins and CDKs genes. Microarray-based studies suggest that induction of p21 is correlated with the suppression of genes involved in cell cycle progression, such as *CDK1* (Chang et al., 2000), *CCNB1*, *CCNB2* and *CDK2* (Ferrandiz et al., 2012).

In addition to the cytostatic activity of R-GNT, we also observe cytotoxicity by inducing cell death by apoptosis in HB4a and MCF-7 cells. MCF-7 cells exhibited greater resistance to cell death induced by goniothalamin relative to HB4a cells. Consistent with our study, breast cancer MDA-MB-231 cells exposed to GNT (30 μM) have been reported to exhibit an increase in the population of apoptotic cells with mitochondrial efflux of cytochrome-c and activation of the effector caspase-3 (Chen et al., 2005). The induction of cell death by apoptosis is one of the most established mechanisms of action for GNT, and other authors have reported its potential to induce apoptosis (Alabsi et al., 2013; Barcelos et al., 2014; Kuo et al., 2011; Petsophonsakul et al., 2013). Most studies report that apoptosis induced by GNT occurs through by intrinsic pathway, with activation of initiator caspase-9 (Alabsi et al., 2013; Inayat-Hussain et al., 2003), decrease in mitochondrial membrane potential, and mitochondrial release of cytochrome-c (Kuo et al., 2011) and of SMAC/DIABLO (Petsophonsakul et al., 2013). Some reports also suggest that the extrinsic pathway participates in GNT-induced apoptosis, as demonstrated by the activation of the initiator caspase of the extrinsic pathway, caspase-8 (Kuo et al., 2011; Petsophonsakul et al., 2013). The caspase initiator-2 (Chan et al., 2010) and the caspases effector-3 and -7 have been activated by goniothalamin exposure (Al-Qubaisi et al., 2013; Inayat-Hussain et al., 1999). However, in this study, there was no differential gene expression of *CASP8* and *CASP9*, the genes that are encoded to caspase-8 and to caspase-9, respectively. S-GNT, unlike R-GNT, exhibited low cytotoxicity and did not induce cell death by apoptosis in MCF-7 cells. There is a report that this enantiomer induced cell death mainly by autophagy in kidney 786-O cells (de Fatima et al., 2008). However, S-GNT at 50 μM was able to induce apoptosis in HB4a cells.

5. Conclusion

In summary, in the current study, we observed the potent antiproliferative activity of goniothalamin against breast cell lines in a dose- and time-dependent manner. Indeed, there was no selective cytotoxicity for MCF-7 tumor cells relative to HB4a non-tumor cells. The natural enantiomer R-GNT proved most effective for both cell lines relative to the synthetic enantiomer S-GNT. R-GNT can inhibit cell proliferation via cell cycle arrest and apoptosis induction, likely in response to DNA damage and upregulation of *GADD45a* gene. R-GNT induced G0/G1 and G2/M cell cycle arrest in MCF-7 cells, according to the concentration, as well as G2/M cell cycle arrest in HB4a cells. The cell cycle inhibition induced by R-GNT was mediated by the upregulation of CIP/KIP cyclin-kinase inhibitors and by the downregulation of cyclins and CDKs. S-GNT, in turn, was able to induce G0/G1 cell cycle arrest and DNA damage in MCF-7 cells and to induce apoptosis only in HB4a cells. Therefore, goniothalamin presents potent antiproliferative activity to breast cancer cell line MCF-7 in a dose- and time-dependent manner. However, exposure to this goniothalamin brings some undesirable effects to non-

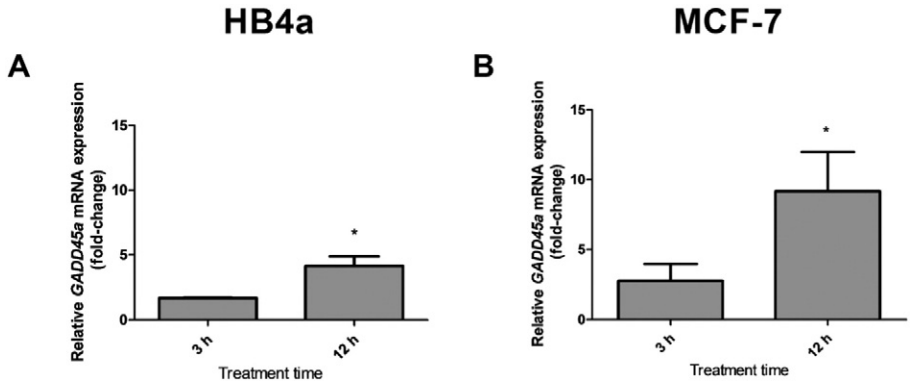

Fig. 9. RT-qPCR analysis of Growth Arrest and DNA Damage (Gadd) 45a gene (GADD45a). Graphs shown the relative gene expression (fold-change in (A) HB4a and (B) MCF-7 cells after 3 h and 12 h of exposure to R-GNT 50 μM. The relative expression of target gene was normalized with the reference genes Glyceraldehyde 3-phosphate dehydrogenase (GAPDH). Data are expressed as fold changes relative to control group in three independent experiments (mean ± SEM). Statistical differences compared to Control are indicated by * (REST 2009 software ®).

tumor cells HB4a, including genotoxicity and apoptosis induction, and further studies are needed to clarify their potential toxic effects.

Transparency document

The Transparency document associated with this can be found, in online version.

References

Abassi, Y.A., Xi, B., Zhang, W., Ye, P., Kirstein, S.L., Gaylord, M.R., Feinstein, S.C., Wang, X., Xu, X., 2009. Kinetic cell-based morphological screening: prediction of mechanism of compound action and off-target effects. Chem Biol 16, 712–723.

Abbas, T., Dutta, A., 2009. p21 in cancer: intricate networks and multiple activities. Nat. Rev. Cancer 9, 400–414.

Al-Qubaisi, M., Rosli, R., Subramani, T., Omar, A.R., Yeap, S.K., Ali, A.M., Alitheen, N.B., 2013. Goniothalamin selectively induces apoptosis on human hepatoblastoma cells through caspase-3 activation. Nat. Prod. Res. 27, 2216–2218.

Al-Qubaisi, M., Rozita, R., Yeap, S.K., Omar, A.R., Ali, A.M., Alitheen, N.B., 2011. Selective cytotoxicity of goniothalamin against hepatoblastoma HepG2 cells. Molecules 16, 2944–2959.

Alabsi, A.M., Ali, R., Ali, A.M., Al-Dubai, S.A., Harun, H., Abu Kasim, N.H., Alsalahi, A., 2012. Apoptosis induction, cell cycle arrest and in vitro anticancer activity of gonothalamin in a cancer cell lines. Asian Pac J Cancer Prev 13, 5131–5136.

Alabsi, A.M., Ali, R., Ali, A.M., Harun, H., Al-Dubai, S.A., Ganasegeran, K., Alshagga, M.A., Salem, S.D., Abu Kasim, N.H., 2013. Induction of caspase-9, biochemical assessment and morphological changes caused by apoptosis in cancer cells treated with goniothalamin extracted from *Goniothalamus macrophyllus*. Asian Pac J Cancer Prev 14, 6273–6280.

Barcelos, R.C., Pastre, J.C., Vendramini-Costa, D.B., Caixeta, V., Longato, G.B., Monteiro, P.A., de Carvalho, J.E., Pilli, R.A., 2014. Design and synthesis of N-acylated Aza-goniothalamin derivatives and evaluation of their in vitro and in vivo antitumor activity. ChemMedChem 9, 2725–2743.

Besson, A., Dowdy, S.F., Roberts, J.M., 2008. CDK inhibitors: cell cycle regulators and beyond. Dev. Cell 14, 159–169.

Brandimarto, J.A., 2009. Molecular regulation of insulin-like growth factor binding protein-5 by signaling molecules downstream of the IGF-I receptor in mammary epithelial cells. State University of New Jersey, p. 61.

Castaneda, F., Rosin-Steiner, S., 2006. Low concentration of ethanol induce apoptosis in HepG2 cells: role of various signal transduction pathways. Int J Med Sci 3, 160–167.

Chan, K.M., Rajab, N.F., Siegel, D., Din, L.B., Ross, D., Inayat-Hussain, S.H., 2010. Goniothalamin induces coronary artery smooth muscle cells apoptosis: the p53-dependent caspase-2 activation pathway. Toxicol. Sci. 116, 533–548.

Chang, B.D., Watanabe, K., Broude, E.V., Fang, J., Poole, J.C., Kalinichenko, T.V., Roninson, I.B., 2000. Effects of p21Waf1/Cip1/Sdi1 on cellular gene expression: implications for carcinogenesis, senescence, and age-related diseases. Proc. Natl. Acad. Sci. U. S. A. 97, 4291–4296.

Chen, W.Y., Wu, C.C., Lan, Y.H., Chang, F.R., Teng, C.M., Wu, Y.C., 2005. Goniothalamin induces cell cycle-specific apoptosis by modulating the redox status in MDA-MB-231 cells. Eur. J. Pharmacol. 522, 20–29.

Cheung-Ong, K., Giaever, G., Nislow, C., 2013. DNA-damaging agents in cancer chemotherapy: serendipity and chemical biology. Chem Biol 20, 648–659.

Collins, A.R., Oscoz, A.A., Brunborg, G., Gaivao, I., Giovannelli, L., Kruszewski, M., Smith, C.C., Stetina, R., 2008. The comet assay: topical issues. Mutagenesis 23, 143–151.

de Fatima, A., Kohn, L.K., Antonio, M.A., de Carvalho, J.E., Pilli, R.A., 2005. (R)-goniothalamin: total syntheses and cytotoxic activity against cancer cell lines. Bioorg. Med. Chem. 13, 2927–2933.

de Fatima, A., Zambuzzi, W.F., Modolo, L.V., Tarsitano, C.A., Gadelha, F.R., Hyslop, S., de Carvalho, J.E., Salgado, I., Ferreira, C.V., Pilli, R.A., 2008. Cytotoxicity of goniothalamin enantiomers in renal cancer cells: involvement of nitric oxide, apoptosis and autophagy. Chem. Biol. Interact. 176, 143–150.

Eroles, P., Bosch, A., Perez-Fidalgo, J.A., Lluch, A., 2012. Molecular biology in breast cancer: intrinsic subtypes and signaling pathways. Cancer Treat. Rev. 38, 698–707.

Fatima, A., Kohn, L.K., Carvalho, J.E., Pilli, R.A., 2006. Cytotoxic activity of (S)-goniothalamin and analogues against human cancer cells. Bioorg. Med. Chem. 14, 622–631.

Ferrandiz, N., Caraballo, J.M., Garcia-Gutierrez, L., Devgan, V., Rodriguez-Paredes, M., Lafita, M.C., Bretones, G., Quintanilla, A., Munoz-Alonso, M.J., Blanco, R., Reyes, J.C., Agell, N., Delgado, M.D., Dotto, G.P., Leon, J., 2012. p21 as a transcriptional co-repressor of S-phase and mitotic control genes. PLoS One 7 (e37759).

Gartel, A.L., Tyner, A.L., 1999. Transcriptional regulation of the p21((WAF1/CIP1)) gene. Exp. Cell Res. 246, 280–289.

Hanahan, D., Weinberg, R.A., 2011. Hallmarks of cancer: the next generation. Cell 144, 646–674.

Inayat-Hussain, S.H., Annuar, B.O., Din, L.B., Ali, A.M., Ross, D., 2003. Loss of mitochondrial transmembrane potential and caspase-9 activation during apoptosis induced by the novel styryl-lactone goniothalamin in HL-60 leukemia cells. Toxicol. in Vitro 17, 433–439.

Inayat-Hussain, S.H., Osman, A.B., Din, L.B., Ali, A.M., Snowden, R.T., MacFarlane, M., Cain, K., 1999. Caspases-3 and -7 are activated in goniothalamin-induced apoptosis in human Jurkat T-cells. FEBS Lett. 456, 379–383.

Inayat-Hussain, S.H., Wong, L.T., Chan, K.M., Rajab, N.F., Din, L.B., Harun, R., Kizilors, A., Saxena, N., Mourtada-Maarabouni, M., Farzaneh, F., Williams, G.T., 2009. RACK-1 overexpression protects against goniothalamin-induced cell death. Toxicol. Lett. 191, 118–122.

Jin, S., Antinore, M.J., Lung, F.D., Dong, X., Zhao, H., Fan, F., Colchagie, A.B., Blanck, P., Roller, P.P., Fornace Jr., A.J., Zhan, Q., 2000. The GADD45 inhibition of Cdc2 kinase correlates with GADD45-mediated growth suppression. J Biol Chem 275, 16602–16608.

Jin, S., Tong, T., Fan, W., Fan, F., Antinore, M.J., Zhu, X., Mazzacurati, L., Li, X., Petrik, K.L., Rajasekaran, B., Wu, M., Zhan, Q., 2002. GADD45-induced cell cycle G2–M arrest associates with altered subcellular distribution of cyclin B1 and is independent of p38 kinase activity. Oncogene 21, 8696–8704.

Kuo, K.K., Chen, Y.L., Chen, L.R., Li, C.F., Lan, Y.H., Chang, F.R., Wu, Y.C., Shiue, Y.L., 2011. Involvement of phorbol-12-myristate-13-acetate-induced protein 1 in goniothalamin-induced TP53-dependent and -independent apoptosis in hepatocellular carcinoma-derived cells. Toxicol. Appl. Pharmacol. 256, 8–23.

Lee, J., Kim, J.A., Barbier, V., Fotedar, A., Fotedar, R., 2009. DNA damage triggers p21WAF1-dependent Emi1 down-regulation that maintains G2 arrest. Mol. Biol. Cell 20, 1891–1902.

Li, Y., Qian, H., Li, X., Wang, H., Yu, J., Liu, Y., Zhang, X., Liang, X., Fu, M., Zhan, Q., Lin, C., 2009. Adenoviral-mediated gene transfer of Gadd45a results in suppression by inducing apoptosis and cell cycle arrest in pancreatic cancer cell. J Gene Med 11, 3–13.

Macleod, K.F., Sherry, N., Hannon, G., Beach, D., Tokino, T., Kinzler, K., Vogelstein, B., Jacks, T., 1995. p53-dependent and independent expression of p21 during cell growth, differentiation, and DNA damage. Genes Dev. 9, 935–944.

Malumbres, M., Barbacid, M., 2005. Mammalian cyclin-dependent kinases. Trends Biochem. Sci. 30, 630–641.

Malumbres, M., Barbacid, M., 2009. Cell cycle, CDKs and cancer: a changing paradigm. Nat. Rev. Cancer 9, 153–166.

Mosmann, T., 1983. Rapid colorimetric assay for cellular growth and survival: application to proliferation and cytotoxicity assays. J. Immunol. Methods 65, 55–63.

Musgrove, E.A., Caldon, C.E., Barraclough, J., Stone, A., Sutherland, R.L., 2011. Cyclin D as a therapeutic target in cancer. Nat. Rev. Cancer 11, 558–572.

Nigg, E.A., 2001. Mitotic kinases as regulators of cell division and its checkpoints. Nat Rev Mol Cell Biol 2, 21–32.

Petsophonsakul, P., Pompimon, W., Banjerdpongchai, R., 2013. Apoptosis induction in human leukemic promyelocytic HL-60 and monocytic U937 cell lines by goniothalamin. Asian Pac J Cancer Prev 14, 2885–2889.

Pfaffl, M.W.H.,.G.W., Dempfle, L., 2002. Relative expression software tool (REST©) for group-wise comparison and statistical analysis of relative expression results in real-time PCR. Nucleic Acids Res. 30, 1–10.

Pihie, A.H., Stanslas, J., Din, L.B., 1998. Non-steroid receptor-mediated antiproliferative activity of styrylpyrone derivative in human breast cancer cell lines. Anticancer Res. 18, 1739–1743.

Rajab, N.F., Zariyantey, A.H., Hassan, H., Ali, A.M., Din, L.B., Inayat-Hussain, S.H., 2005. Evaluation of the cytotoxic and genotoxic effects of goniothalamin in leukemic cell lines. Environ. Mutagen. Res. 27, 161–164.

Romanov, V.S., Pospelov, V.A., Pospelova, T.V., 2012. Cyclin-dependent kinase inhibitor p21(Waf1): contemporary view on its role in senescence and oncogenesis. Biochemistry (Mosc) 77, 575–584.

Semprebon, S.C., de Fatima, A., Lepri, S.R., Sartori, D., Ribeiro, L.R., Mantovani, M.S., 2014. (S)-goniothalamin induces DNA damage, apoptosis, and decrease in BIRC5 messenger RNA levels in NCI-H460 cells. Hum Exp Toxicol 33, 3–13.

Sugaya, S., Nakanishi, H., Tanzawa, H., Sugita, K., Kita, K., Suzuki, N., 2005. Down-regulation of SMT3A gene expression in association with DNA synthesis induction after X-ray irradiation in nevoid basal cell carcinoma syndrome (NBCCS) cells. Mutat. Res. 578, 327–332.

Tamura, R.E., de Vasconcellos, J.F., Sarkar, D., Libermann, T.A., Fisher, P.B., Zerbini, L.F., 2012. GADD45 proteins: central players in tumorigenesis. Curr Mol Med 12, 634–651.

Tian, Z., Chen, S., Zhang, Y., Huang, M., Shi, L., Huang, F., Fong, C., Yang, M., Xiao, P., 2006. The cytotoxicity of naturally occurring styryl lactones. Phytomedicine 13, 181–186.

Tice, R.R., Agurell, E., Anderson, D., Burlinson, B., Hartmann, A., Kobayashi, H., Miyamae, Y., Rojas, E., Ryu, J.C., Sasaki, Y.F., 2000. Single cell gel/comet assay: guidelines for in vitro and in vivo genetic toxicology testing. Environ. Mol. Mutagen. 35, 206–221.

Tucker, G.T., 2000. Chiral switches. Lancet 355, 1085–1087.

Vendramini-Costa, D.B., de Castro, I.B., Ruiz, A.L., Marquissolo, C., Pilli, R.A., de Carvalho, J.E., 2010. Effect of goniothalamin on the development of Ehrlich solid tumor in mice. Bioorg. Med. Chem. 18, 6742–6747.

Wang, X.W., Zhan, Q., Coursen, J.D., Khan, M.A., Kontny, H.U., Yu, L., Hollander, M.C., O'Connor, P.M., Fornace Jr., A.J., Harris, C.C., 1999. GADD45 induction of a G2/M cell cycle checkpoint. Proc. Natl. Acad. Sci. U. S. A. 96, 3706–3711.

Wattanapiromsakul, C., Wangsintaweekul, B., Sangprapan, P., Itharat, A., Keawpradub, N., 2005. Goniothalamin, a cytotoxic compound, isolated from *Goniothalamus macrophyllus* (Blume) Hook. f. &Thomson var. *macrophyllus*. Songklanakarin. J. Sci. Technol 27, 479–487.

WHO, World Health Organization-, 2012. GLOBOCAN 2012. Estimated cancer incidence mortality and prevalence worldwide in 2012.

Wiart, C., 2007. Goniothalamus species: a source of drugs for the treatment of cancers and bacterial infections? Evid Based Complement Alternat Med 4, 299–311.

Xing, J.Z., Zhu, L., Jackson, J.A., Gabos, S., Sun, X.J., Wang, X.B., Xu, X., 2005. Dynamic monitoring of cytotoxicity on microelectronic sensors. Chem Res Toxicol 18, 154–161.

Zhou, Q., Stetler-Stevenson, M., Steeg, P.S., 1997. Inhibition of cyclin D expression in human breast carcinoma cells by retinoids in vitro. Oncogene 15, 107–115.